Spectrochimica Acta Part A: Molecular and Biomolecular Spectroscopy 122 (2014) 451–460

Contents lists available at ScienceDirect

Spectrochimica Acta Part A: Molecular and Biomolecular Spectroscopy

journal homepage: www.elsevier.com/locate/saa

Physicochemical properties of liposomes as potential anticancer drugs carriers. Interaction of etoposide and cytarabine with the membrane: Spectroscopic studies

Danuta Pentak *

Department of Materials Chemistry and Chemical Technology, Institute of Chemistry, University of Silesia, 40-006 Katowice, Poland

HIGHLIGHTS

- Liposomes containing tested drugs can be obtained by mREV method.
- Liposomes containing Ara-C and VP-16-213 can be used in cancer therapy.
- Main phase transition temperature T_C can be determined from ^{1}H NMR spectra.

GRAPHICAL ABSTRACT

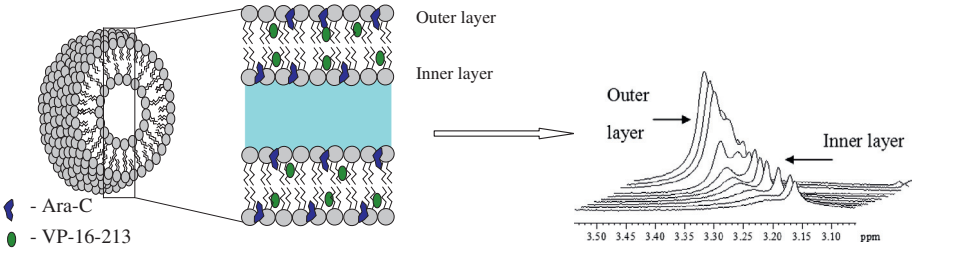

ARTICLE INFO

Article history:
Received 1 October 2013
Received in revised form 5 November 2013
Accepted 10 November 2013
Available online 21 November 2013

Keywords:
Liposome
VP-16-213
Ara-C
NMR
AFM
DSC

ABSTRACT

The interactions between etoposide, cytarabine and 1,2-dihexadecanoyl-*sn*-glycerol-3-phosphocholine bilayers were studied using differential scanning calorimetry (DSC), Fourier transform infrared spectroscopy (FT-IR) and nuclear magnetic resonance (NMR). These techniques have proven to be a very powerful tool in studying the structure and dynamics of phospholipid bilayers. In particular, DSC can provide information on the phase transition temperature and cooperativity of the lipid molecules in the absence and presence of the drug. Vibrational spectroscopy is well suited to the study of drug–lipid interactions, since it allows for an investigation of the conformation of phospholipid molecules at different levels in lipid bilayers and follows structural changes that occur during the gel to liquid–crystalline phase transition. NMR supported the determination of the main phase transition temperatures (T_C) of 1,2-dihexadecanoyl-*sn*-glycerol-3-phosphocholine (DPPC). The main phase transition temperature (T_C) determined by ^{1}H NMR is comparable with values obtained by DSC for all studied liposomes. The location of cytarabine and etoposide in liposomes was also determined by NMR. Atomic force microscopy (AFM) images, acquired immediately after sample deposition on a mica surface, revealed the spherical shape of lipid vesicles.

Introduction

In the past decade, liposomes have been extensively used in research, analytical and therapeutic applications [1]. Liposomes are micro- or nano-particle vesicles formed by self-assembly of natural (phospholipids, cholesterol, etc.) or synthetic amphiphiles in an aqueous environment. They are formed by concentric lipid bilayers surrounding aqueous compartments [2]. First categorized by Bangham et al. [3] on the basis of size, liposomes are described as small unilamellar vesicles (SUV; 20–100 nm), large unilamellar vesicles (LUV; 50–400 nm) and multilamellar vesicles (MLV; 400–5000 nm). Frequently prepared using non-toxic phospholipids and cholesterol, they are biodegradable, biocompatible and non-immunogenic [4,5]. Their structure is similar to that of cells and thus they can be used as a more easily characterizable vessel for studying interactions between membrane lipids and biomolecules such as DNA [6], proteins [7] and drugs [8].

Considering the nature of the drug and the liposomal composition, both hydrophilic and hydrophobic compounds can interact

* Tel.: +48 32 3591446.
E-mail address: danuta.pentak@us.edu.pl

1386-1425/$ - see front matter © 2013 Elsevier B.V. All rights reserved.
http://dx.doi.org/10.1016/j.saa.2013.11.061

with liposomes in different ways; they can be incorporated into the bilayer membrane, adsorbed on the surface, anchored at the polar head group region or entrapped in the aqueous core [9].

The objective of this study was to evaluate the physicochemical properties of liposomes that accommodate hydrophobic and amphiphilic drugs used in cancer therapy. The studied liposomes were prepared using the modified reverse-phase evaporation method (mREV). Thermotropic transitions in liposomal membranes were observed.

The analyzed compounds were 1-β-D-arabinofuranosylcytosine (cytarabine, Ara-C, amphiphilic properties) and etoposide (VP-16-213, hydrophobic properties) (Fig. 1).

The examined drugs are used in various therapies, including doxorubicin, methylprednisolone, high-dose cytarabine, cisplatinum (ASHAP) [10]; cytarabine, cyclophosphamide, tioguanine (BACT) [11]; vincristine, cytarabine, methotrexate (BVAM) [12]; carboplatin, etoposide, cyclophosphamide (CEC) [13]; dexamethasone, ifosfamide, cisplatin, etoposide (DICE) [14]; etoposide, methotrexate, dactinomycin, vincristine, and cyclophosphamide (EMACO) [15].

A combination of the above agents is used in doxorubicin, methotrexate, vincristine, prednisone, leucovorin, cytarabine, cyclophosphamide, etoposide (AMOPLACE) [16]; etoposide, cytarabine, melphalan (BEAM) [17]; methotrexate, vincristine, prednisone, cytarabine, cyclophosphamide, etoposide (MOPLACE) [18]; Mprednisone, methotrexate (high-dose), doxorubicin, cyclophosphamide, etoposide, cytarabine, bleomycin, vincristine, and methotrexate (ProMACE-CytaBOM) [19] therapies.

Etoposide (VP-16-213) (Fig. 1) is one of the most successful chemotherapeutic agents used for the treatment of human cancers. The drug is currently in its third decade of clinical use and is a front line therapy for a variety of malignancies, including leukaemias, lymphomas and several solid tumors [20]. It is a topoisomerase-II inhibitor that acts through the activation of oxidation–reduction reactions that produce derivatives that bind directly to DNA and cause DNA damage [21]. Etoposide has a short biological half-life (3.6 h), with a terminal half-life of 1.5 h intravenously and a variable oral bioavailability ranging from 24% to 74%. Although intraperitoneal injection would result in initial high local tumor concentrations, prolonged exposure of tumor cells may not be possible. The tumoricidal effects of etoposide incorporated into lipid nanoparticles after a single-dose administration showed stronger and prolonged apoptotic induction properties, resulting in a higher increase in the survival time of tumor bearing mice [22].

Cytarabine (Ara-C) (Fig. 1) is an effective chemotherapeutic agent for the treatment of acute myelogenous leukaemia and lymphocytic leukaemia [23]. It has often been utilised in combination chemotherapy, against solid tumours and leukaemias.

Cytarabine is a nucleoside analogue of deoxycytidine in which the ribose sugar has been replaced with an arabinose sugar. Cytarabine penetrates cells by a carrier-mediated process that is shared with other nucleosides [24]. As cytarabine is a cell cycle-dependent drug, prolonged exposure of cells to cytotoxic concentrations is critical to achieve maximum cytotoxic activity. *In vitro* studies suggest that maximum cytotoxic activity is achieved with administration of cytarabine to reach concentrations $\geqslant$0.1 mg/L that are maintained for at least 24 h [25].

Keeping in mind the harmful and even destructive effects of the cytostatic drugs on healthy body cells, it is necessary to search for new delivery methods for these drugs.

There are many articles describing the results of investigations of incorporation of cytarabine [26] and etoposide [27] into

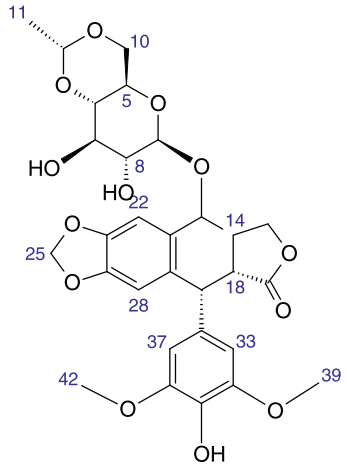

Etoposide (VP-16-213)

4′-Demethylepipodophyllotoxin 9-(4,6-O-ethylidene-β-D-glucopyranoside)

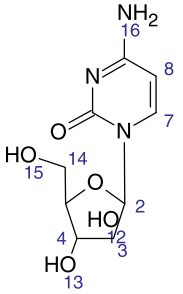

Cytarabine (Ara-C)

1-β-D-arabinofuranosylcytosine

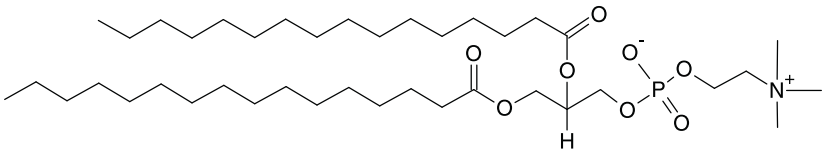

DPPC

1,2-dihexadecanoyl-*sn*-glycerol-3-phosphocholine

Fig. 1. Structures and assignments of the investigated drugs and DPPC.

liposome vesicles. However, there is no information about their simultaneous incorporation, in spite of the fact that these two drugs have been used for more than 30 years.

A number of phospholipids may be used to manufacture liposomes, which may be broadly classified into natural phospholipids (e.g. phosphatidylcholine (PC), phosphatidylserine and phosphatidylglycerol from egg yolk or soya beans and sphingomyelin) and synthetic phospholipids (e.g. distearoylphosphatidylcholine (DSPC) dipalmitoylphosphatidylcholine (DPPC), dimyristoylphosphatidylcholine (DMPC) and dilaurylphosphatidylcholine (DLPC)) [28].

The choice of the type of phospholipid is important for an application of liposomes as drug carriers [29]. 1,2-Dihexadecanoyl-*sn*-glycerol-3-phosphocholine (DPPC) is the most frequently used among synthetic phospholipids. Liposomes obtained from DPPC exhibit higher stability and leak tightness in a wider temperature range. It has been found that the maximum penetration of phospholipid membranes takes place around the main phase transition temperature (T_C) [30]. This is connected with the release of the drug transported by the liposome [31]. The main phase transition temperature (T_C) of DPPC is 41 °C [32].

Traditional temperature-sensitive liposomes require relatively high temperatures (42–45 °C) to induce drug release [33]. Temperatures in this range are not readily achievable throughout the tumor volume in a clinical setting because of patient pain during heating and the potential for normal tissue injury [34]. In contrast, low temperature-sensitive liposomes release their contents at 39–42 °C. This temperature range is readily achievable for superficial and even deep-seated tumors [35].

The size of liposomes, as well as the lipid composition, affects their circulation in the blood [36]. During the last decade, a great deal of basic information on the accumulation of liposomes in tumors has been reported. It has been shown that liposomes are able to cross vessel walls in a tumor [37], and that the size and blood circulation of liposomes affect their ability to accumulate in tumors [38]. In addition it has been shown that the antitumor activity and toxicity of a liposomal antitumor drug are dependent on the size of the liposome carriers [39]. These facts suggest that the size of a liposome may be a key determinant in elevating the targeting efficiency of liposomes aimed at tumor tissues and in designing more effective liposomal antitumor drugs [40].

This study was performed in order to estimate the location and competition between the analyzed drugs for encapsulation in liposome vesicles. The applied methods were nuclear magnetic resonance (NMR), atomic force microscopy (AFM), differential scanning calorimetry (DSC) and Fourier transform infrared spectroscopy (FT-IR). All of the tested methods supported investigations of liposome/drug system formation by analyzing the signals assigned to each drug.

Materials and methods

Materials

L-α-phosphatidylcholine dipalmitoyl (1,2-dihexadecanoyl-*sn*-glycerol-3-phosphocholine) (DPPC, purity 99%), 1-β-D-arabinofuranosylcytosine (cytarabine, Ara-C), 4′-Demethylepipodophyllotoxin 9-(4,6-O-ethylidene-β-D-glucopyranoside) (etoposide, VP-16-213), formaldehyde solution, dimethyl sulfoxide were purchased from Sigma–Aldrich, Schnelldorf, Germany. Chloroform, dichloromethane, hydrochloric acid and phosphate buffered saline (PBS buffer pH 7.4: K_2HPO_4, NaH_2PO_4) were supplied by POCH, Gliwice, Poland. Deuterium oxide (D_2O) 99%, dimethyl sulfoxide-d_6 99.96 atom% D, chloroform-*d* 99%, stab. with Ag and sodium 4,4-dimethyl-4-silapentane sulfonate (DSS) were purchased from ARMAR Chemicals, Döttingen, Switzerland.

Methods

Liposome preparation

Small liposomes (DPPC, DPPC/Ara-C, DPPC/VP-16-213, DPPC/Ara-C/VP-16-213, were obtained by the modified reverse-phase evaporation method (mREV) [41]. PBS buffer with pH 7.4 was applied. For ^{1}H NMR and FT-IR measurements, 5×10^{-3} M VP-16-213 in DMSO-d_6 and 5×10^{-3} M Ara-C in D_20 were added to the preparation mixture.

For DSC and AFM, 5×10^{-3} M VP-16-213 in DMSO and 5×10^{-3} M Ara-C in H_20 were added to the preparation mixture. The preparation process was carried out at 44 °C. Liposome entrapped Ara-C, VP-16-213 were separated from free Ara-C, VP-16-213 by dialysis in a Servapor dialysis tubing with several changes of buffer at 4 °C.

Nuclear magnetic resonance

All spectra were obtained by the 9.4 Tesla Bruker Avance Ultra-Shield (400.130 MHz for ^{1}H) (Karlsruhe, Germany) with the use of a 5 mm inverse broadband probe (BBI). ^{1}H NMR spectra were recorded at a temperature range of 25–47 °C. 2D NOESY spectra were recorded at 47 °C. Sample temperature was controlled by air and monitored by the Bruker thermal control system. The samples were heated at a rate of up to 1.0 °C min^{-1} and were left for approximately 20 min to achieve equilibrium which was monitored based on the free induction decay (FID) signal. The temperature was maintained at ±0.1 °C. Water suppression was obtained by presaturation. 32 Transients were accumulated with ^{1}H pulse length of 10.70 μs and 5 s relaxation delay, 2.044 s acquisition time, 32,768 date points and 0.30 Hz line broadening. ^{1}H chemical shift values were referred to DSS as an external reference. The spectra were processed with the use of TopSpin 3.1 (Bruker, Karlsruhe) software. Apparatus error was ± 0.001 ppm.

Differential scanning calorimetry

Differential scanning calorimetry (DSC) scans were performed using the VP DSC ultrasensitive microcalorimeter (MicroCal Inc., Northampton, MA) with 0.5 mL cell volume. Degassing during the calorimetric experiments was prevented by additional constant pressure of 1.8 atm over the liquids in the cells. At first, the buffer was placed in both the sample and reference compartments. A DSC curve corresponding to buffer vs. buffer run was used as the instrumental baseline. The calorimetric data were corrected for the calorimetric baseline (by subtracting buffer – buffer scan). Heat capacity vs. temperature profiles were obtained for a scanning rate of 1.0 °C min^{-1} at a temperature of 10–65 °C. A minimum of at least three heating scans were performed for each analysis and all thermograms were reproducible. The Origin 6.0 software package was used to evaluate the transition temperatures (maximum of each peak) and the transition enthalpies ΔH (area under each peak).

Fourier transform infrared spectroscopy

Fourier transform infrared spectra were obtained using a PerkinElmer Spectrum One FT-IR spectrometer (Waltham, MA) equipped with a IF KT-3 (Krakow, Poland) automatic temperature controller. Spectra were recorded for both dried and full hydrated samples of liposomes. For the dried samples spectra were recorded at room temperature. The lipid dispersions were placed in a demountable cell between two ZnSe windows which were separated by a 50-μm thick Teflon spacer. For temperature regulation, the cell was placed in a thermostatized jacket with internal temperature measurement. An external water bath was used for

temperature control. The temperature was maintained at ±0.1 °C. All the spectra were acquired after equilibrate of the liposomes samples for 15 min at each desired temperature ranging from 16 °C to 50 °C using automatic temperature controller. Data acquisition was performed every 2 °C. For each spectrum, covering the 3000–800 cm^{-1} region, 10 interferograms were coadded, apodized and Fourier transformed to give a resolution of 2 cm^{-1}. Moreover, FT-IR spectrum of buffer was also obtained under identical instrumental conditions. Peak positions were determined with one significant digits with Spectrum v3.01 spectral processing software.

Atomic force microscopy

Atomic force microscopy (AFM) images were obtained in ambient conditions using the Multimode Nanoscope IIIa system (Digital Instruments, USA). Surface morphology was measured with tapping mode AFM at room temperature. Height and phase imaging data were acquired simultaneously using a commercial silicon tip-cantilever with stiffness of around 40 Nm^{-1}. Height and phase images were obtained, and all scans were performed with scan frequency below 1.00 Hz in air.

AFM images were obtained by measuring interaction forces between the tip and the sample surface. Immediately before the analysis, the samples were diluted in 1% formaldehyde solution (1:100) to lower analyte viscosity. Constant-volume droplets (40 μl) were deposited onto a small mica disk with the diameter of 1 cm. The study was performed immediately after the preparation. The height and diameter of liposomes were measured from the profile section of AFM line scans analyzing height images.

Results and discussion

Differential scanning calorimetry study

The aim of the DSC study was to examine the effect of temperature on liposome membranes composed of DPPC, DPPC/Ara-C, DPPC/VP-16-213, and DPPC/Ara-C/VP-16-213. DSC scans clearly show two endothermic transitions. Table 1 presents the parameters calculated from DSC traces of DPPC liposomes containing cytarabine and etoposide and Fig. 2 shows examples of these traces.

The low-temperature peak at ~34 °C was regarded as the pre-transition (T_P) peak. The tall and sharp maximum temperature peak was indicative of main phase transition (T_C) at a temperature of ~41 °C. Two discernible transitions were observed, and three lamellar phases ($L_{\beta'}$, $P_{\beta'}$ and L_α) were determined for all DPPC bilayers within the temperature range of 10–65 °C under ambient pressure. $L_{\beta'}$, $P_{\beta'}$ and L_α represented tilted gel, ripple gel and liquid–crystalline phases, respectively. Pre-transitions and main phase transitions were thus ascribed to $L_{\beta'} \rightarrow P_{\beta'}$ and $P_{\beta'} \rightarrow L_\alpha$ phase transitions, respectively. The recorded transition temperatures and enthalpies are in good agreement with literature value [32,42].

Unfortunately, a phase sub-transition was not observed. Most probably, the 10-h sample incubation time at 4 °C was too short

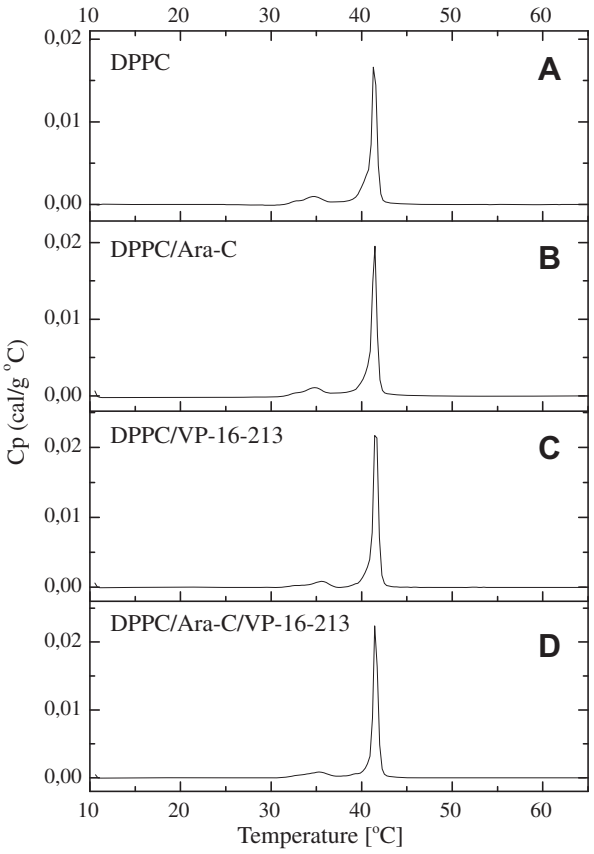

Fig. 2. Differential scanning calorimetry traces of dipalmitoylphosphatidylcholine liposomes containing different drugs. Control is DPPC liposomes.

and did not allow for an observation of the sub-transition from the crystalline subgel (L_C) phase to the tilted gel ($L_{\beta'}$) phase [43]. In the subgel phase (L_C) the hydrocarbon chains are in a fully extended, all-*trans* conformation and the polar head groups are relatively immobile [44]. A sub-transition has been described for DPPC with a T_m of 21.5 °C [32]. Two processes occur upon formation of the L_C phase from the $L_{\beta'}$ phase: a dehydration of the polar head group and a rearrangement of the acyl chains from a quasi-hexagonal to a more ordered packing. Koynova and Tenchov [43] demonstrated that for 16:0/16:0 PC these two processes take place in discrete steps upon cooling. The $L_{\beta'}$ phase first converts to the so-called sub-subgel (SGII) phase with well-ordered acyl chains but with the same lamellar repeat period as the $L_{\beta'}$ phase. This conversion is rapidly reversible and presumably proceeds without significant change in hydration state. The SGII–$L_{\beta'}$ transition is referred to as the sub-sub-transition. The formation of the stable L_C phase, presumably involving the dehydration step, takes place from within the SGII phase upon equilibration. Thus, the formation

Table 1
Values of phase pre-transition (T_P) and main transition (T_C) temperatures, half-width temperature and enthalpy changes ΔH of dipalmitoylphosphatidylcholine liposomes containing different drugs as assessed by differential scanning calorimetry.

Liposome/drug	Pre-transition			Main transition		
	T_P (°C)	$\Delta T_{1/2}$ (°C)	ΔH (cal/g)	T_C (°C)	$\Delta T_{1/2}$ (°C)	ΔH (cal/g)
DPPC	34.64 ± 0.21	3.46 ± 0.04	2.10 ± 0.05	41.30 ± 0.12	0.79 ± 0.01	10.26 ± 0.04
DPPC/Ara-C	34.82 ± 0.33	2.93 ± 0.07	2.30 ± 0.05	41.47 ± 0.14	0.53 ± 0.01	10.84 ± 0.05
DPPC/VP-16-213	35.54 ± 0.31	3.21 ± 0.08	2.22 ± 0.04	41.42 ± 0.11	0.79 ± 0.01	11.62 ± 0.07
DPPC/Ara-C/VP-16-213	35.30 ± 0.25	3.48 ± 0.06	1.79 ± 0.05	41.45 ± 0.11	0.79 ± 0.01	9.97 ± 0.06

T_P – pre-transition temperature; T_C – main transition temperature; $\Delta T_{1/2}$ – the temperature width at half peak height; ΔH – the transition enthalpy. The data represented the mean ± S.D. ($n \geqslant 3$).

of the SGII phase appears to be an intermediate step in the process of L_C phase formation which proceeds as follows: $L_{\beta'} \rightarrow$ SGII $\rightarrow L_C$. The time required to fully convert the metastable SGII phase to the stable L_C phase during low temperature incubation is chain length-dependent. Thus, for example, conversion times can vary from 30 min in the case of 10:0/10:0 PC to more than 10 days for 16:0/16:0 PC and $\geqslant$1.5 years in the case of the 21:0/21:0 PC and 22:0/22:0 PC [42].

In the present study, for all drug-containing liposomes, an insignificant increase in the pre-transition and main phase transition temperature was observed (Table 1).

El Maghraby et al. [45] postulated that the pre-transition (T_P) can be due to rotation of the phospholipid head groups or to conformational changes in the phospholipid bilayer structure. The highly ordered gel state (L_β) with the hydrocarbon chains in an all-*trans* configuration (tilted one-dimensional arrangement) changes to a two dimensional arrangements with periodic undulations (rippled gel phase, P_β). This means that any compound that interacts with the head groups will affect the pre-transition. The authors also postulated that the $\Delta T_{1/2}$ parameter is very sensitive to the presence of any additives.

The largest changes in the values of the $\Delta T_{1/2}$ parameter were obtained for liposomes composed of DPPC/Ara-C (which may suggest the changes in co-operativity that were postulated by El Maghraby and can indicate interaction at the interface site).

Apart from the observed changes in $\Delta T_{1/2}$ values for liposomes composed of DPPC/Ara-C, all the other changes in the sub-phase transition and the main phase transition for the remaining liposomes are within experimental error, indicating that the analyzed drugs do not significantly affect the temperature of phase transitions.

Keeping in mind the character of the studied drugs and the changes in the values of the $\Delta T_{1/2}$ parameter, it may be presumed that in the case of cytarabine, an adsorption takes place at the water–lipid bilayer interface with some degree of penetration into bilayer. On the other hand, strongly lipophilic drugs such as etoposide are located in the bilayer.

Fourier transform infrared spectroscopy

Infrared spectra of liposomes

Fourier transform infrared spectroscopy (FT-IR) has been established as an efficient spectroscopic method for biochemical analysis of biological samples. In this study, FT-IR spectroscopy was employed to examine the effects of cytarabine and etoposide on the conformation of lipid acyl chains as well as headgroup and interfacial regions. Spectra of dried samples were recorded at room temperature. Spectra of control and drug-loaded liposomes over the 3000–800 cm^{-1} range are shown in Fig. 3, and frequencies of selected absorption bands are listed in Table 2.

Absorption bands considered to yield the most useful information for the analysis of FT-IR spectra are: methylene asymmetric and symmetric stretching, carbonyl stretching, and phosphate asymmetric and symmetric stretching modes. It is well known that in the methylene stretching region of the infrared spectrum (3000–2800 cm^{-1}), hydrocarbon chains which contain *gauche* conformers absorb infrared radiation at higher frequencies than those which contain all-*trans* conformers. Thus, increases in hydrocarbon chain conformational disorder (however caused) are accompanied by increases in the frequencies of infrared absorption bands arising from the symmetric and asymmetric stretching vibrations of the methylene groups in lipid hydrocarbon chains. This property can thus be used to as a general-purpose monitor of changes in lipid hydrocarbon chain conformational disorder and has frequently been used for the detection and/or monitoring of lipid hydrocarbon chain-melting phase transitions [46,47].

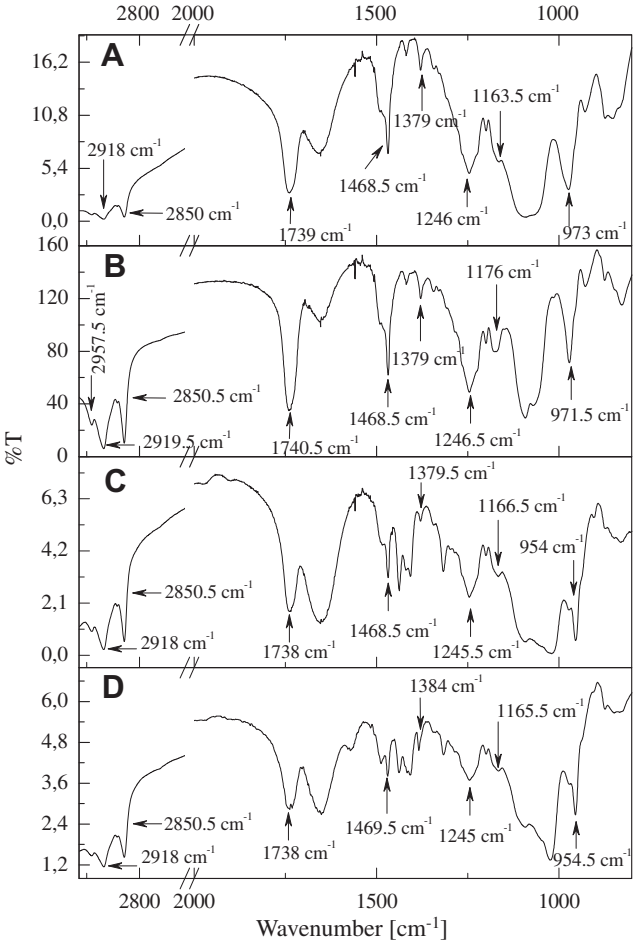

Fig. 3. FT-IR spectra of (A) control DPPC liposomes; (B) DPPC/Ara-C; (C) DPPC/VP-16-213; and (D) DPPC/Ara-C/VP-16-213 liposomes.

Table 2
Assigned bands of the FT-IR spectra of dried samples of DPPC, DPPC/Ara-C, DPPC/VP-16-213, DPPC/Ara-C/VP-16–213 liposomes.

Vibrational mode	Frequency (cm^{-1})			
	DPPC	DPPC/Ara-C	DPPC/VP-16-213	DPPC/Ara-C/VP-16-213
ν_{as} (CH_3)	2958.0	2957.5	2957.5	2958.0
ν_{as} (CH_2)	2918.0	2919.5	2918.0	2918.0
ν_s (CH_2)	2850.0	2850.5	2850.5	2850.5
ν (C=O)	1739.0	1740.5	1738.0	1738.0
CH_2 scissoring	1468.5	1468.5	1468.5	1469.5
CH_2 wagging	nd	nd	1317.0	1316.5
δ_s (CH_3)	1379.0	1379.0	1379.5	1384.0
ν_{as} (P=O)	1246.0	1246.5	1245.5	1245.0
ν_s (OC—O)	1163.5	1176.0	1166.5	1165.5
ν_{as} (N—CH_3)	973.0	971.5	954.0	954.5

ν – Stretching band; δ – bending band; as – asymmetric; s – symmetric; nd – not detected.

In the spectral region of 3000–2800 cm^{-1} for all obtained liposomes, the acyl chain methylene C–H bond asymmetric stretching ν_{as} (CH_2) and symmetric stretching ν_s (CH_2) modes were observed at 2919.5–2918 cm^{-1} and 2850.5–2850 cm^{-1}, respectively. There was no significant influence of cytarabine and etoposide in obtained liposomes on FT-IR spectra over 2000 cm^{-1} (Table 2). The most dominant features are in the 1400–800 cm^{-1} region.

Useful information regarding acyl chain packing and inter-chain interactions is derived from CH_2 scissoring and wagging modes.

The CH_2 scissoring and wagging bands of the extended acyl chains of DPPC are located in the regions of 1480–1460 cm^{-1} and 1350–1180 cm^{-1}, respectively, being characteristic of the nature of acyl chain packing in the gel phase. There were no significant changes in the scissoring band observed at ~1468.5 cm^{-1} for all obtained liposomes. It is significant that the wagging band at ~1317 cm^{-1} was observed only in liposomes containing etoposide. Ausborn et al. [48] have reported that in liposomes, new absorption is visible when interactions between molecules are changed. These results indicate that the acyl chains of DPPC are influenced by the etoposide in DPPC/VP-16-213 and DPPC/Ara-C/VP-16-213 liposomes.

Additionally, there was a N–CH_3 stretching band of DPPC at 973 cm^{-1} in control liposomes. The asymmetric N–CH_3 stretching band at 973 cm^{-1} is from the choline group in DPPC. This band was observed at 971.5 cm^{-1}, 954 cm^{-1} and 954.5 cm^{-1} in DPPC/Ara-C, DPPC/VP-16–213, DPPC/Ara-C/VP-16–213 liposomes, respectively. These results indicate that the choline group of DPPC is influenced by the drugs incorporated in liposomes.

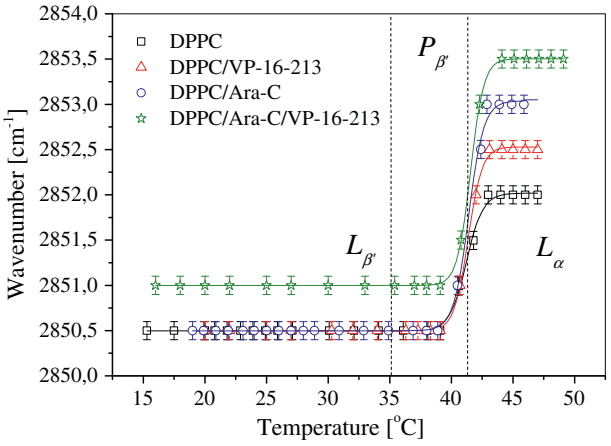

Fig. 4. Comparison of the temperature-dependency of the peak position of the CH_2 symmetric stretching band of studied liposomes at the $L_{\beta'}$, $P_{\beta'}$ and L_{α} phase transitions of the lipid; temperature range 15–47 °C.

Studies of lipid phase transitions

Fourier transform infrared spectroscopy is particularly useful for measuring phospholipid phase transitions. Investigations of phase transition temperature profiles of lipids are crucial to understanding various phenomena such as conformational order or disorder, transmembrane diffusion, vesicle formation and fusion as well as drug-membrane interactions. In order to find the T_C, temperature, spectra of DPPC liposomes containing drugs and not containing drugs were obtained for between 3000–2800 cm^{-1}, the region where CH_2 vibrations in hydrocarbon chains are strongest. It is well known that the frequencies of CH_2 stretching modes depend on the chain conformational disorder of the hydrocarbon tail [49,50]. The conformational disordering of an all-*trans* hydrocarbon chain is accompanied not only by an upward shift in the ν_s (CH_2) and ν_{as} (CH_2) IR band maxima, but also by a significant broadening of the overall band envelope. These changes reflect the increase in hydrocarbon chain conformational disorder and mobility that occurs with the onset of *gauche* rotamer formation and the concomitant decline in the number of all-*trans* rotamers present upon chain melting. Although most spectroscopists have used the CH_2 asymmetric stretching band (~2920 cm^{-1}) as a precursor for order–disorder phenomena [46,47], in this study it is shown that the symmetric stretching band (~2850 cm^{-1}) also produces similar results.

The tests were performed in the 15–47 °C temperature range. With increasing temperature the vibrational frequency (or wavenumber) of these bands increased abruptly in all studied samples as they passed through the gel to liquid crystalline transition temperature (Fig. 4).

The temperature-dependent changes in the symmetric CH_2 stretching band allowed for a determination of the phase transition temperature T_C for all the studied liposomes (Table 3). The results that were obtained are in agreement with literature [51] and clearly show the three different phase regions of $L_{\beta'}$, $P_{\beta'}$ and L_{α}. This method, which allows for determining the main phase transition temperature (T_C), is based on calculating the second derivative of the observed temperature changes.

In this case, the determined main phase transition temperatures (T_C) for DPPC, DPPC/Ara-C, DPPC/VP-16-213 and DPPC/Ara-C/VP-16-213 liposomes are 41.28 ± 0.1 °C, 41.52 ± 0.1 °C, 41.46 ± 0.1 °C and 41.50 ± 0.1 °C, respectively. Finally, the results originating from infrared spectroscopy for phase transitions of studied liposomes agree to within less than 0.5 °C with values obtained from the DSC method.

Table 3
Comparative main phase transition temperature, T_C (°C) profiles for DPPC, DPPC/Ara-C, DPPC/VP-16-213 and DPPC/Ara-C/VP-16-213 liposomes obtained from different techniques.

Liposome	DSC (°C)	FT-IR (°C)	^{1}H NMR (°C)
DPPC	41.30 ± 0.12	41.28 ± 0.1	41.71 ± 0.1
DPPC/Ara-C	41.47 ± 0.14	41.52 ± 0.1	42.07 ± 0.1
DPPC/VP-16-213	41.42 ± 0.11	41.46 ± 0.1	41.91 ± 0.1
DPPC/Ara-C/VP-16-213	41.45 ± 0.11	41.50 ± 0.1	42.15 ± 0.1

Nuclear magnetic resonance study

NMR spectroscopy is a powerful non-destructive technique for studying biomembranes. 2D NOESY is very useful for structural determination because its presence indicates that the two nuclei are undergoing dipole–dipole cross-relaxation, and are therefore in close proximity to one another (<5 Å) [52].

Two-dimensional NOE, or nuclear Overhauser effect spectroscopy (NOESY), allows simultaneous connectivity of all protons in the spectrum to be established. Instead of saturation, the two-dimensional technique involves inversion of proton resonances and observation of the resulting free induction decay. The resulting spectrum is represented in a two-dimensional map, with each axis corresponding to a proton chemical shift scale. The standard one-dimensional proton spectrum appears on the diagonal, while NOE enhancements appear as off-diagonal peaks. If two peaks have an off-diagonal NOE peak, they must be in close proximity to one another. Because two-dimensional NOESY allows the connectivity of all protons to be simultaneously established, it is very useful for the study of the structure of complicated biological macromolecules. The one-dimensional technique is, however, quantitatively more accurate [53] and more reliable. Furthermore, one-dimensional experiments are less time-consuming than two-dimensional experiments, and are better suited for study of dilute solutions [54].

^{1}H NMR and NOESY measurements were performed to evaluate the effects of temperature on liposomal membranes and to examine mutual interactions between the analyzed drugs (Ara-C, VP-16-213 (Fig. 1)) and their phospholipid carriers. Liposomes composed of DPPC, DPPC/Ara-C, DPPC/VP-16-213 and DPPC/Ara-C/VP-16-213 were analyzed (Fig. 5).

The effects of temperature on liposome membranes were determined by ^{1}H NMR between 25 and 47 °C. The signal at ~3.15 ppm was assigned to choline head groups. In addition to a temperature-

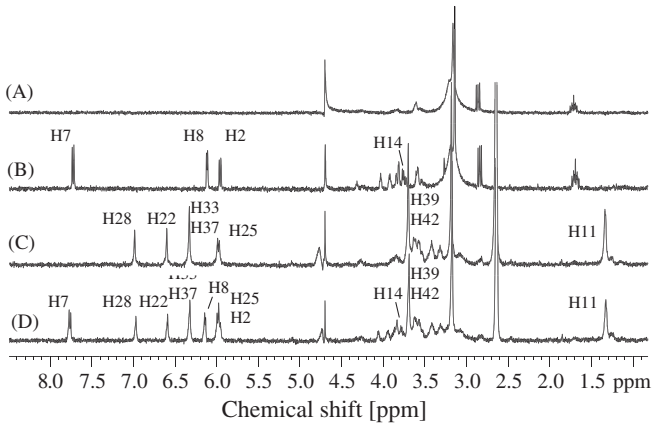

Fig. 5. ^{1}H NMR spectra of liposome: (A) DPPC; (B) DPPC/Ara-C; (C) DPPC/VP-16-213; and (D) DPPC/Ara-C/VP-16-213. ^{1}H NMR spectra of liposomes were recorded at a temperature 25 °C.

induced increase in the intensity of the signal produced by the protons of ammonium methyl groups $-N^+(CH_3)_3$, signal splitting and a minor transition to lower field of the spectrum were also observed (Fig. 6).

As seen in Fig. 6 there exist two separated peaks; one of them appeared at the higher field corresponds to the lipid locating in the inner layer, and the other peak at the lower field comes from the lipid in the outer layer. The choline methyl protons of the lipid in the inner layer resonance at higher magnetic field, while those in the outer layer resonance at lower magnetic field [55]. The reason may be the following. The lipids in the inner layer are more densely packed than the lipids being in the outer layer, leading to a requirement of higher field strength for the resonance. When temperature becomes higher, the difference in the chemical shift between the inner and the outer layers becomes smaller. This can be understood as evidence that an increase in the mobility of the lipid headgroup causes a decrease in the effect of packing density [56,57].

The above mentioned behavior can be attributed to changes in phospholipid distribution in the membrane which take place during three consecutive phases: tilted gel phase ($L_{\beta'}$)), ripple gel phase ($P_{\beta'}$) and liquid–crystalline phase (L_α). Transitions between these phases have not only close biological relevance but also physical chemistry importance [58]. Not all phase transitions observed in DSC thermograms are noted in NMR spectra. An analysis of the $-N^+(CH_3)_3$ signal supports the determination of main phase transition temperature T_C, i.e. the transition from the ripple gel phase ($P_{\beta'}$) to the liquid–crystalline phase (L_α). The estimation of the temperature T_C value uses the sequence of spectra for each thermally equilibrated system as shown in Fig. 6. Fig. 6 shows that increase of temperature leads to an increase of area of the signal of protons of methyl groups of ammonium of phospholipids – $N^+(CH_3)_3$. Practically, the determination can be made through the variation either of the amplitude or of the area of peaks, (DSS was used as an external standard). Derivative of NMR peak area was determined from the signals. The peak maximum shows the phase transition temperature (T_C). The determination of the temperature T_C with the use of ^{1}H NMR is not as convenient as with DSC but allows for determination of the main phase transition of

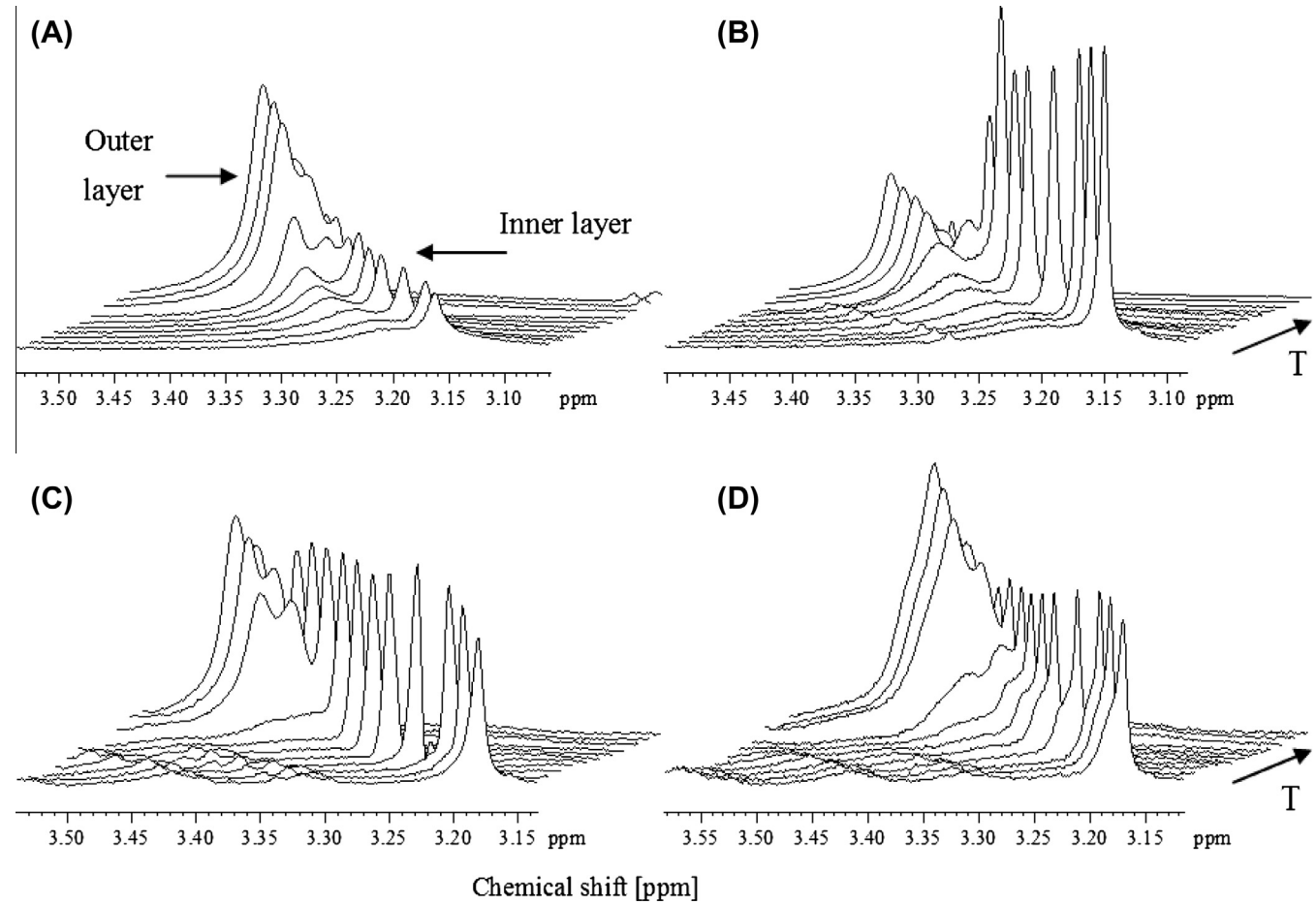

Fig. 6. The effect of temperature on the peaks of $-N^+(CH_3)_3$ choline head group regions at ~3.15 ppm of liposomes composed of: (A) DPPC; (B) DPPC/Ara-C; (C) DPPC/VP-16-213; and (D) DPPC/Ara-C/VP-16-213. ^{1}H NMR spectra of liposomes were recorded at a temperature of 25–47 °C.

Table 4
Chemical shift observed in ^{1}H NMR of selected protons of cytarabine before and after incorporation in liposomes.

Peak assignment	δ (ppm) Ara-C	$\Delta\delta$ (ppm) DPPC/Ara-C	$\Delta\delta$ (ppm) DPPC/Ara-C/VP-16-213
H7	7.592	−0.006	0.032
H8	5.984	−0.006	0.016
H2	5.831	−0.009	0.005
H14	3.622	**−0.014**	**0.030**

Bold text: significant changes. Apparatus error ±0.001 ppm.

Table 5
Chemical shift observed in ^{1}H NMR of selected protons of etoposide before and after incorporation in liposomes.

Peak assignment	δ (ppm) VP-16-213	$\Delta\delta$ (ppm) DPPC/VP-16-213	$\Delta\delta$ (ppm) DPPC/Ara-C/VP-16-213
H28	7.007	−0.168	−0.176
H22	6.529	−0.075	−0.078
H33,37	6.180	0.002	0.003
H25	6.031	**−0.200**	**−0.195**
H39,42	3.325	**−0.230**	**−0.226**
H11	1.242	−0.050	−0.054

Bold text: significant changes. Apparatus error ±0.001 ppm.

phospholipid. The values of T_C for all analyzed liposomes are shown in Table 3.

The proposed method of determination of the main phase transition temperature T_C turns out to be very reproducible. In our previous study this technique was described that can be used to estimate the T_C temperature of phospholipids for liposomes entrapped 5-fluorouracil/leucovorin [59] and 5-fluorouracil/cytarabine [60]. The results are consistent with those obtained by DSC. Terech et al. used similar approach to estimate the phase transition temperatures of 12-hydroxy stearic acid (HSA) in nitrobenzene [61].

In comparison with the DSC method, the greatest differences in the values of T_C were obtained for liposomes composed of DPPC/Ara-C/VP-16-213. These differences amount to 0.7 ± 0.1 °C. The closest values were obtained for liposomes constructed only from DPPC.

To examine the mutual interactions between cytarabine, etoposide and DPPC, ^{1}H NMR tests were performed (Fig. 5). A shift in cytarabine signals toward higher field was observed after incorporating this drug into liposomes (Table 4).

It was determined that the observed changes in chemical shift values of the analyzed signals that originated in H7, H8 (pyrimidine ring), H2 (sugar residue) and H14 protons of cytarabine are the result of a shielding effect caused by an increase in electron densities around the protons. The greatest changes $\Delta\delta$ = −0.014 ppm were observed for H14 protons. A simultaneous incorporation of cytarabine and etoposide into liposomes (competition with the second drug) caused a shift in the analyzed cytarabine signals towards lower field. Also in this case, the greatest changes were observed for H14 protons ($\Delta\delta$ = 0.030 ppm). This may be connected with the deshielding effect caused by the decrease of electron densities around the analyzed protons. This phenomenon points to a formation of hydrogen bonds.

In the case liposomes containing etoposide (Table 5), it can be determined that incorporating the drug into the liposome causes a selective shift in the analyzed signals. H28, H22, H25, H39, H42 and H11 protons were shifted toward higher field. On the other hand, in the case of H33 and H37 protons, the opposite effect was observed – there was a shift toward the lower field. The values of the chemical shifts remained almost unchanged despite the incorporation of a second drug – cytarabine. The greatest changes on the order of 0.200 ppm and 0.230 ppm were observed for H25 and H39, and H42 protons respectively.

In addition, it was observed that after incorporating both drugs into liposomes a similar shift for proton doublets H25 of etoposide and H2 of cytarabine was observed. It can be concluded that the cytarabine pyrimidine ring is probably incorporated into liposome vesicles located in the bilayer region at the same depth as the etoposide ring. The observed changes allow us to suppose that drugs incorporated into liposome vesicles can compete.

2D cross-relaxation spectra of DPPC liposomes that contain and do not contain drugs were obtained to analyze the location of Ara-C and VP-16-213 in liposomes and the mutual interactions between drugs and liposomal phospholipids. In the NOESY spectrum of DPPC/Ara-C/VP-16-213 liposomes, a cross peak between etoposide H22 protons and cytarabine H14 protons was observed ((1) in Fig. 7).

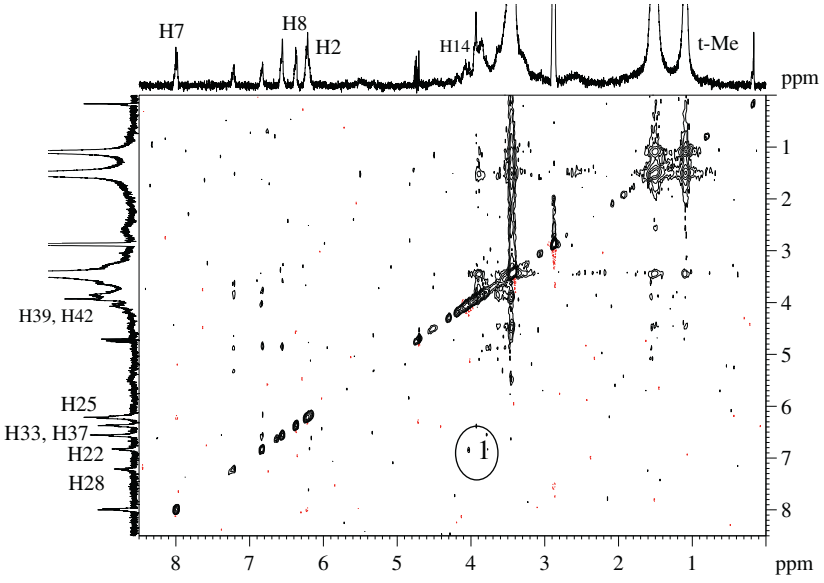

Fig. 7. A 2D NOESY ^{1}H NMR spectrum of DPPC/Ara-C/VP-16-213 liposomes recorded with a mixing time of 500 ms at a temperature of 47 °C. Diagonal peaks correspond to a 1D spectrum. Off-diagonal peaks represent magnetization transfer between protons. Such transfers occur between adjacent lipid molecules and drug molecules, and they are indicative of lipid matrix disorders resulting from a temperature increase.

Table 6
Mean height and diameter of liposomes obtained by AFM.

Types of liposomes	Height (nm)	Diameter (nm)
DPPC	2.04 ± 0.22	100.40 ± 5.12
DPPC/Ara-C	8.29 ± 0.69	74.76 ± 8.60
DPPC/VP-16-213	4.28 ± 0.34	55.22 ± 9.25
DPPC/Ara-C/VP-16-213	7.24 ± 0.62	83.45 ± 6.18

The data represented the mean ± S.D. ($n \geqslant 5$).

The presence of a cross-peak representing the interactions between cytarabine H14 protons and etoposide H22 (1) suggests that cytarabine H14 protons and etoposide H22 protons are situated in the same region of the liposomal membrane, and the distance between them does not exceed 5 Å. The signal in the 2D spectrum confirms the encapsulation of etoposide and cytarabine in liposomes and their mutual interactions.

Atomic force microscopy analysis

AFM is a rapid, powerful and relatively non-invasive technique for analyzing liposome morphology, size and size distribution. The geometry, size and properties of liposomes have to be described to enable potential applications of liposome systems as drug carriers. Tapping mode AFM supports observations of liposome morphology without sample manipulation such as staining, labeling or fixation. The tip only intermittently contacts the surface of the sample, which eliminates the damaging effects of lateral and shear forces on the sample [62]. AFM, a high resolution technique for characterizing materials at the nanometer scale and in real time, works well in air or fluid.

AFM images were obtained of all prepared liposomes. The study was performed immediately after the preparation. The obtained results showed that the size of investigated liposomes depends on the number of encapsulated drugs. The smallest size was observed for liposomes containing one drug (55–75 nm DPPC/VP-16-213; DPPC/Ara-C) and it increased when two drugs were encapsulated simultaneously (83.45 ± 6.18 nm DPPC/Ara-C/VP-16-213) (Table 6).

After deposition, it was observed flat disks in heavy smaller heights than diameters. The topographical changes could be influence by different factors; in fact as the medium droplet suspending liposomes evaporates, liposomes collapse. Also, substrate interaction determines the stability of the vesicles on the mica surface; both composition and size of the liposomes influence the adsorption on the mica layer and then the vesicle deformation. The other possible factor is tip effect. The elastic properties of the lipids constituting liposomes influence the interaction with the tip. The non-contact mode is less likely to damage the sample than the contact mode. This fact was due to the elimination of the lateral force between the sample and the tip. Nevertheless, the vertical force applied by the tip on the liposomes during the scanning procedure induced soft vesicle deformation. Thus, liposomes appear intact only few minutes after deposition on the mica support; their structural changes are influenced by all above-mentioned factors and result in the formation of the flat disks similar to the planar vesicles [63] or pancake-like vesicles as reported previously [64].

The results of presented experiment are consistent with other research findings [65].

Conclusion

The results of this study indicate that the mREV method supports the encapsulation of amphiphilic and hydrophobic drugs in liposomes. The prepared liposomes had a diameter of 55.22 ± 9.25–100.40 ± 5.12 nm. The discussed method for determining the main phase transition temperature T_C based on ^{1}H NMR spectra poses an alternative to DSC. The phase transition temperatures obtained from temperature-induced infrared spectroscopy were compared with DSC as well as NMR results and were found to be in close agreement.

From these results it is possible to conclude that an effective interaction between cytarabine and etoposide and the lipid bilayer is observed and that this interaction does not induce significant changes in the structure of the membrane. Consequently, the physicochemical data suggest that it is possible to obtain stable preparations of liposomes containing cytarabine and etoposide for use in cancer therapy.

Acknowledgement

This study was supported by the State Committee for Scientific Research in Poland (N N204 139039).

References

[1] K.A. Edwards, A.J. Baeumner, Talanta 68 (2006) 1421–1431.
[2] S. Chatterjee, D.K. Banerjee, Methods Mol. Biol. 199 (2002) 3–16.
[3] A.D. Bangham, M.M. Standish, J.C. Watkins, J. Mol. Biol. 13 (1965) 238–252.
[4] M. Voinea, M. Simionescu, J. Cell. Mol. Med. 6 (2002) 465–474.
[5] B. Ruozi, G. Tosi, E. Leo, M.A. Vandelli, Talanta 73 (2007) 12–22.
[6] M. Angelova, I. Tsoneva, Chem. Phys. Lipids 101 (1999) 123–137.
[7] A. Fischer, T. Oberholzer, P. Luisi, Biochim. Biophys. Acta 1467 (2000) 177–188.
[8] D.C. Drummond, O. Meyer, D. Papahadjopoulos, Pharmacol. Rev. 51 (1999) 691–743.
[9] C. Grabielle-Madelmont, S. Lesieur, M. Ollivon, J. Biochem. Biophys. Meth. 56 (2003) 189–217.
[10] H. Nückel, J. Dürig, U. Dührsen, Ann. Hematol. 82 (2003) 481–486.
[11] T. Philip, P. Biron, I. Philip, Eur. J. Cancer Clin. Oncol. 19 (1993) 1371–1379.
[12] E.M. Bessell, F. Graus, J.A. Punt, J. Clin. Oncol. 14 (1996) 945–954.
[13] M. Federico, S. Luminari, E. Iannitto, G. Polimeno, J. Clin. Oncol. 27 (2009) 805–811.
[14] P. Goss, F. Shepherd, J.G. Scott, M. Baker, Leuk Lymphoma 18 (1995) 123–129.
[15] M. Quinn, J. Murray, M. Friedlander, Aust N Z J Obstet Gynaecol 34 (1994) 90–92.
[16] B.A. Parker, M. Santarelli, J. Clin. Oncol. 11 (1993) 248–254.
[17] R. Chopra, A.K. McMillan, D.C. Linch, S. Yuklea, Blood 81 (1993) 1137–1145.
[18] P. Schulman, K. McCarroll, M.R. Cooper, L. Norton, Med. Pediatr. Oncol. 18 (1990) 482–486.
[19] L.J. Swinnen, G.M. Mullen, T.J. Carr, Blood 86 (1995) 3333–3340.
[20] K.R. Hande, Eur. J. Cancer 34 (1998) 1514–1521.
[21] M. Chamberlain, J. Neurooncol. 15 (1993) 133–139.
[22] L.H. Reddy, J.S. Adhikari, B.S.R. Dwarakanath, R.K. Sharma, AAPS J. 8 (2006) E254–E262.
[23] G. Gahrton, Adv. Cancer Res. 40 (1983) 255–329.
[24] J.S. Wiley, S.P. Jones, W.H. Sawyer, J. Clin. Invest. 69 (1982) 479–489.
[25] F.L. Graham, G.F. Whitmore, Cancer Res. 30 (1970) 2627–2635.
[26] A. Hamada, T. Kawaguchi, M. Nakano, Clin. Pharmacokinet 41 (2002) 705–718.
[27] S. Sengupta, P. Tyagi, Pharmacology 62 (2001) 163–171.
[28] K.M.G. Taylor, R.M. Moris, Thermochim. Acta 248 (1995) 289–301.
[29] E. Mastrobattista, G.A. Koning, G. Storm, Adv. Drug. Del. Rev. 40 (1999) 103–127.
[30] F. Frezard, Braz. J. Med. Biol. Res. 32 (1999) 181–189.
[31] V.P. Torchilin, Eur. J. Pharm. Sci. 11 (2000) S81–S91.
[32] Ch. Huang, S. Li, Biochim. Biophys. Acta 1422 (1999) 273–307.
[33] M.H. Gaber, N.Z. Wu, K. Hong, S.K. Huang, M.W. Dewhirst, D. Papahadjopoulos, Int. J. Radiat. Oncol. Biol. Phys. 36 (1996) 1177–1187.
[34] R. Ben-Yosef, D.S. Kapp, Int. J. Hyperthermia 8 (1992) 733–745.
[35] J. Overgaard, D. Gonzalez, M.C. Hulshof, Int. J. Hyperthermia 25 (2009) 323–334.
[36] R.M. Abra, C.A. Hunt, Biochim. Biophys. Acta 666 (1981) 493–503.
[37] D. Papahadjopoulos, T.M. Allen, A. Gabizon, M.C. Woodle, D.D. Lasic, Proc. Natl. Acad. Sci. USA 88 (1991) 11460–11464.
[38] K. Uchiyama, A. Nagayasu, Y. Yamagiwa, T. Nishida, H. Harashima, H. Kiwada, Int. J. Pharm. 121 (1995) 195–203.
[39] L.D. Mayer, L.C.L. Tai, D.S.C. Ko, D. Masin, R.S. Ginsberg, P.R. Cullis, M.B. Bally, Cancer Res. 49 (1989) 5922–5930.
[40] A. Nagayasu, K. Uchiyama, H. Kiwada, Adv. Drug. Del. Rev. 40 (1999) 75–87.
[41] D. Pentak, A. Sułkowska, W.W. Sułkowski, J. Mol. Struct. 887 (2008) 187–193.
[42] R. Koynova, M. Caffrey, Biochim. Biophys. Acta 1376 (1998) 91–145.
[43] R. Koynova, B.G. Tenchov, S. Todinova, P.J. Quinn, Biophys. J. 68 (1995) 2370–2375.
[44] M. Kinoshita, K. Ito, S. Kato, Chem. Phys. Lipids 163 (2010) 712–719.
[45] G.M.M. El Maghraby, A.C. Williams, B.W. Barry, Int. J. Pharm. 292 (2005) 179–185.

[46] R.N.A.H. Lewis, R.N. McElhaney, Biophys. J. 64 (1993) 1081–1096.
[47] R.N.A.H. Lewis, R.N. McElhaney, Biochim. Biophys. Acta 1828 (2013) 2347–2358.
[48] M. Ausborn, H. Schreier, G. Brezeinski, H. Fabian, J. Controlled Release 30 (1994) 105–116.
[49] K.J. Seu, L.R. Cambrea, R.M. Everly, J.S. Hovis, Biophys. J. 91 (2006) 3727–3735.
[50] L. Terminassiansaraga, E. Okamura, J. Umemura, T. Takenaka, Biochim. Biophys. Acta 946 (1988) 417–423.
[51] R.K. Bista, R.F. Bruch, A.M. Covington, Biopolymers 93 (2010) 403–417.
[52] A. Saran, S. Srivastava, E. Coutinho, J. Mol. Struct. 382 (1996) 23–31.
[53] G.M. Clore, A.M. Gronenborn, J. Magn. Reson 61 (1985) 158–164.
[54] A.M. Mathur, A.B. Scranton, Biomaterials 17 (1996) 547–557.
[55] G.L. Jendrasiak, R. Smith, A.A. Ribeiro, Biochim. Biophys. Acta 1145 (1993) 25–32.
[56] L. Michaelis, P. Schlieper, FEBS Lett. 147 (1982) 40–44.
[57] Z. Zhou, Y. Okumura, J. Sunamoto, Proc. Japan Acad. 72 (1996) 23–27.
[58] S. Qin, Z. Yu, Y. Yu, J. Phys. Chem. B 113 (2009) 8114–8123.
[59] D. Pentak, A. Sułkowska, W.W. Sułkowski, Mol. Cryst. Liq. Cryst. 523 (2010) 282–288.
[60] D. Pentak, W.W. Sułkowski, A. Sułkowska, J. Therm. Anal. Calorim. 108 (2012) 67–71.
[61] P. Terech, C. Rossat, F. Volino, J. Colloid Interface Sci. 227 (2000) 363–370.
[62] T.R. Albrecht, P. Grutter, D. Horne, D. Rugard, J. Appl. Phys. 69 (1991) 668–673.
[63] Z.V. Leonenko, A. Carnini, Biochim. Biophys. Acta – Biomembranes 1509 (2000) 131–147.
[64] T. Shibata-Sekia, J. Masai, T. Tagawa, Thin Solid Films 273 (1996) 297–303.
[65] X. Liang, G. Mao, Colloids Surf. B Biointerfaces 34 (2004) 42–51.